Journal of Thermal Analysis and Calorimetry (2021) 145:3077–3085
https://doi.org/10.1007/s10973-020-09886-3

Calorimetric (DSC) and dielectric (TSDC) investigation on the thermal behavior and molecular mobility in the supercooled liquid and glassy states of bifonazole and lamotrigine

Joaquim J. Moura Ramos[1] · **Hermínio P. Diogo**[1]

Received: 8 November 2019 / Accepted: 26 May 2020 / Published online: 17 June 2020

Abstract
The thermal behavior of the two glass-forming drugs bifonazole and lamotrigine was studied by differential scanning calorimetry (DSC); we reported a bifonazole polymorph not yet described in the literature, as well as weak evidence for lamotrigine polymorphism; still by DSC we investigated the glass-forming ability, the tendency for crystallization from the glass (glass stability) from the metastable and equilibrium melt, for the two glass-formers under analysis. Finally, this technique was used to characterize the glass transition of the two active pharmaceutical ingredients by determining the activation energy of the structural relaxation, the dynamic fragility and the heat capacity jump associated with the glass transformation. Using thermally stimulated depolarization currents (TSDC) and, on the other hand, different aspects of the molecular mobility of these glass-formers were analyzed; the glass transition relaxation and the dynamic fragility, as well as the secondary mobility of the two glass-forming systems, were characterized by this dielectric technique. The absence of other dynamic studies on these glass-formers does not allow the comparison of our results with those of other techniques, namely with dielectric spectroscopy; however, despite this, attention was drawn to the general need to understand in their mutual relationship the TSDC and DRS results on the secondary relaxations.

Keywords DSC · Thermostimulated currents · Glass transition · Dynamic fragility · Amorphous solid state · API

Introduction

With this work, we wish to contribute to the understanding of the phase transformations and molecular mobility in two glass-forming active pharmaceutical ingredients (APIs): bifonazole and lamotrigine. Bifonazole is an imidazole-based anti-fungal agent with broad spectrum activity against many fungi, molds, yeast and some Gram-positive bacteria [1]. Lamotrigine is an anticonvulsant medication introduced for treatment of seizure disorders and now used to treat epilepsy and bipolar disorder [2]. The research presented here is not, however, intended to address the medical applications of these substances, but rather to study the thermodynamic and kinetic properties upon which their stability and bioavailability depend. Modern medicines are fascinating from a molecular point of view because of the huge diversity of their chemical structures and dimensions, which gives them a great diversity of physical and chemical properties and behaviors, and justifies their frequent polymorphism. Many of them are also good glass-formers displaying a wide range of glass-forming abilities and glass stabilities. This diversity and richness of molecular behaviors gives rise to an increased interest in the study of their different phases and respective interconversions.

In the pharmaceutical field, the amorphous form of drugs is often preferred over crystalline because of the higher solubility and dissolution rate that result from its higher Gibbs energy [3–6]. However, the amorphous solid tends to crystallize (decrease in the Gibbs energy), tendency which depends in particular on two factors: the degree of molecular mobility [7–10] and the thermodynamic driving force for crystallization [11]. Knowledge of the amorphous properties

Electronic supplementary material The online version of this article (https://doi.org/10.1007/s10973-020-09886-3) contains supplementary material, which is available to authorized users.

✉ Hermínio P. Diogo
hdiogo@tecnico.ulisboa.pt

[1] CQE – Centro de Química Estrutural, Complexo I, Instituto Superior Técnico, Universidade de Lisboa, 1049-001 Lisbon, Portugal

is therefore important for defining the most appropriate stabilization procedures and storage conditions.

Furthermore, unit operations on a large-scale batch such as freeze and spray drying may lead to the generation of amorphous systems, while grinding or conventional drying may result in materials which are partially or wholly disordered. In both situations, diagnosing manufacturing irregularities should be part of a quality protocol.

In this work, we use the techniques of differential scanning calorimetry (DSC) to study phase diagram aspects such as thermodynamic transitions and polymorphism, and to characterize the glass transition, while with thermostimulated depolarization currents (TSDC) we will study the slow molecular mobility in the amorphous solid state, in the glass transition region and in the metastable liquid just above T_g of the two glass-forming systems under study.

Experimental

Materials

Bifonazole, (RS)-1-[phenyl(4-phenylphenyl)methyl]-1H-imidazole or 1-(p,α-diphenylbenzyl)imidazole, with molecular formula $C_{22}H_{18}N_2$, molecular mass 310.39 g mol^{-1} and CAS number 60628-96-8, was provided by TCI, lot number UAVZA-LM with purity of 99.3%.

Lamotrigine, 3,5-diamino-6-(2,3-dichlorophenyl)-1,2,4-triazine, with molecular formula $C_9H_7Cl_2N_5$, molecular mass 256. 094 g mol^{-1} and CAS number 84057-84-1, was provided by Acros, lot number A0374231 with G.P. ≥ 98%.

The chemical structures of these substances are shown in Fig. 1; the acquired samples were used without further purification.

Techniques

Differential scanning calorimetry (DSC)

The calorimetric measurements were performed with a 2920 MDSC system from TA Instruments Inc. The samples with ~ 5.0 mg mass were contained in aluminum pans sealed in air. All the measurements were done under helium (Air Liquide N55), at a flow rate of 30 cm^3 min^{-1}. Details of the experimental procedures and of the calibration of the temperature and heat flow scales are presented elsewhere [12]. All weightings were performed with a precision of ± 0.1 μg in a Mettler UMT2 ultra-micro balance.

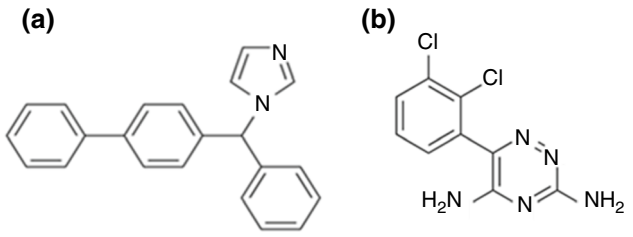

Fig. 1 Molecular structures of **a** bifonazole and **b** lamotrigine

Thermally stimulated depolarization currents (TSDC)

Thermally stimulated depolarization current experiments were carried out with a TSC/RMA spectrometer (TherMold, Stamford, CT, USA) covering the range from − 170 to + 400 °C. A clear and concise explanation of the experimental procedures provided by the technique of thermally stimulated currents is available (see Supplementary data associated with Ref. [13]) and may be useful for the reader unfamiliar with this technique.

The temperature-dependent relaxation time, $\tau(T)$, associated with a given TSDC peak can be calculated using methods described in the literature (supplementary data associated with Ref. [13] or appendix of Ref. [14]). The physical foundations of the TSDC technique are exposed in different classic books [15–17], while its applications are explained in several reviews [18–22].

To prepare the sample for the TSDC experiments, ~ 30 mg of the as-received crystalline powder were placed on the lower electrode of the TSDC equipment, introduced into an oven and then melted under vacuum (at T = 165 °C for bifonazole and at T = 235 °C for lamotrigine). The lower electrode/sample assembly was then cooled to room temperature and transferred at normal pressure to the TSC cell, where it was mounted with the upper electrode (7 mm diameter) to form the parallel plate capacitor (thickness of ~ 0.5 mm). Three successive vacuum/helium cycles allowed the TSDC cell to be placed under a helium atmosphere of 1.1 bar and, prior to the experimental measurements, the sample was heated up to the metastable liquid to improve electrical contact with both electrodes (at T = 40 °C for bifonazole and at T = 110 °C for lamotrigine).

Results and discussion

Differential scanning calorimetry

General thermal behavior and polymorphism

Bifonazole The as-received sample displayed a DSC endothermic peak with maximum at $(T_{fus})_{max}$ = 148.7 °C at 10 °C min^{-1} (onset at $(T_{fus})_{on}$ = 145.6 °C), and the corresponding melting enthalpy was ΔH_{fus} = 38.49 kJ mol^{-1}, in good agreement with the published values (see Table 1).

Table 1 Melting temperature, T_{fus}, and enthalpy of fusion, ΔH_{fus}, of the studied API glass-formers

	T_{fus}/°C		ΔH_{fus}/kJ mol^{-1}	
	This work	Literature	This work	Literature
Bifonazole	148.7	148.8[a]; 149 [23, 24]; 150 [25]; 151 [26, 27]; 153 [28]	38.5	32.8 [27]; 34.1 [24]; 36.7 [29]; 37.5 [25]; 39.0 [26]
Lamotrigine	218.0	216 [30]; 217 [31–36]; 220 [37–39]	33.7	35.2 [30]; 38.2 [36]

[a]Certificate of analysis from the manufacturer

Cold crystallization was observed on heating either from the amorphous solid state or from a temperature above T_g (see Fig. 2); at 2.5 °C min^{-1} it starts at ~ 70 °C, has a maximum rate at ~ 90 °C and ends at ~ 110 °C. The crystal produced by cold crystallization shows an endothermic DSC peak at $(T_{fus})_{max} = 148.8$ °C, with an area corresponding to a melting enthalpy of $\Delta H_{fus} = 107.9$ J g^{-1} = 33.50 kJ mol^{-1}; the melting temperature is similar to that of the as-received sample, but the different melting enthalpy suggests that we are in the presence of a metastable polymorph (form II), not yet reported in the literature. We further verified that the melting temperature and enthalpy of the crystalline sample obtained by isothermal crystallization from the metastable liquid at 90 °C are exactly the same as that of the crystal obtained by cold crystallization on heating from the amorphous solid. The sample supplied by the manufacturer, with a higher melting enthalpy and a very close melting temperature, will therefore correspond to the most stable polymorph (form I).

Lamotrigine The as-received sample displayed a DSC endothermic peak with maximum at $(T_{fus})_{max} = 218.0$ °C (onset at $T_{on} = 216.3$ °C), and the corresponding melting enthalpy was $\Delta H_{fus} = 33.7$ kJ mol^{-1}, in reasonable agreement with the values reported in the literature [30, 36] (see Table 1).

No crystallization is observed on cooling from the isotropic liquid; however, cold crystallization is observed starting at $T_{in} \cong 150 \pm 10$ °C and maximum speed at $T_{max} \cong 175 \pm 10$ °C for heating rates between 5 and 15 °C min^{-1} (see Fig. 2). No clear signs of polymorphism were observed in lamotrigine; however, the shape of the endothermic fusion peak often shows an asymmetry (even a slightly noticeable double character) that may indicate the existence of polymorphs with very close melting temperatures.

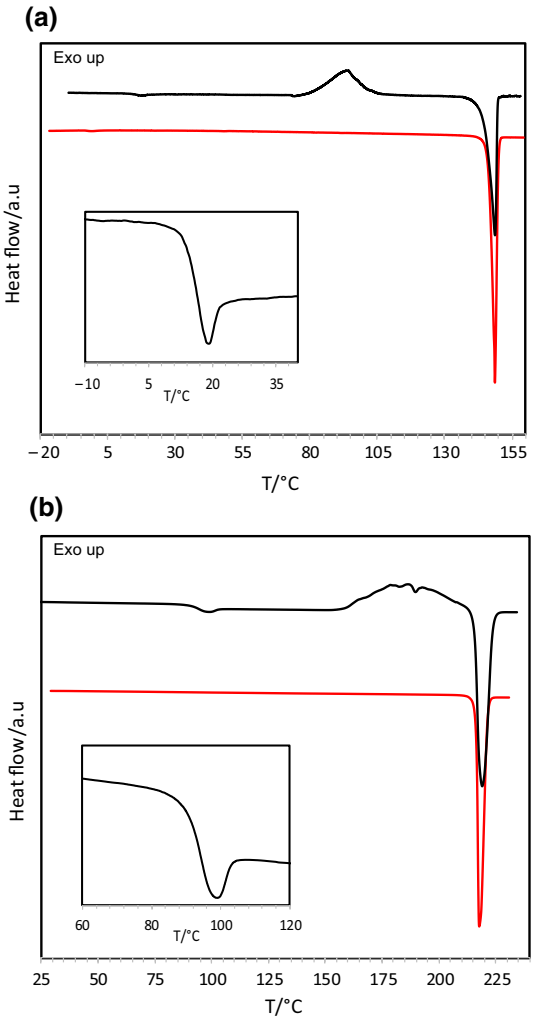

Fig. 2 **a** DSC successive scans on heating at 5 °C min^{-1} for the as-received crystalline form of bifonazole (red line) and for the sample cooled down from the melt down to the glassy state (black line); **b** DSC successive scans on heating at 10 °C min^{-1} for the as-received crystalline form of lamotrigine (red line) and for the sample cooled down from the melt down to the glassy state (black line). In both cases, no crystallization was observed on cooling from the melt down to below T_g; the signature of the cold crystallization is clearly shown and the insert displays the detail of the glass transition step signal

The glass transition and the dynamic fragility

As far as we know, there are no published studies on the molecular mobility in the amorphous solid state and in the glass transition region for either bifonazole or lamotrigine. In this work, we will use two experimental techniques to obtain information in this field, namely to obtain the glass transition temperature, the activation energy of the structural relaxation

and the dynamic fragility for the two glass-formers under study. In this section, we will present results obtained by differential scanning calorimetry, whereas the conclusions of the analysis by thermostimulated depolarization currents will be presented in Section "The glass transformation region".

In the DSC study, we will determine the activation energy of the structural relaxation, $E_a(T_g)$, from the effect of the heating rate on the temperature location of the glass transition step signal [40, 41]:

$$\frac{d(\ln q^+)}{d(1/T_x)} = -\frac{E_a(T_x)}{R}, \quad (1)$$

where q^+ is the heating rate, T_x is the temperature that defines the position of the DSC glass transition step signal, and R is the gas constant. The cooling/heating cycles of the experimental protocol obey the necessary condition that $q^-/q^+ = 1$, i.e., the rate of a given cooling is always equal to that of the next heating [40–42]. In addition, to define the temperature location of the step signal of the glass transition we considered two different temperatures, namely the temperature of the onset, T_{on}, and the temperature of the overshoot, T_{ov}: the latter because it can be determined with greater accuracy and the first, T_{on}, for being the one that as was shown in a recent work [45], is physically more acceptable because it is less affected by physical aging. Therefore, although some authors suggest the use of T_{ov} [43, 44], we will keep in mind that the values of activation energy of the structural relaxation, $E_a(T_g)$, obtained through Eq. (1) based on T_{on} are physically more acceptable.

Once $E_a(T_g)$ is obtained, the dynamic fragility, m, can be estimated by:

$$m = \frac{E_a(T_g)}{2.303 \times RT_g}, \quad (2)$$

where the 10 based logarithm defines a scale of dynamic fragility, m, such that the lower limit (extremely strong glasses) corresponds to $m_{min} = 16$ [46]; we will use Eq. (2) to calculate $m_{DSC}(T_{ov})$ and $m_{DSC}(T_{on})$ for the two glass-formers under analysis.

Bifonazole The glass transition temperature of bifonazole measured by DSC was found at $T_{gDSC} = 13.8$ °C (extrapolated onset on heating at 10 °C min^{-1}), which compares well with the values reported in the literature (see Table 2). On the other hand, the heat capacity jump observed at the glass transition is $\Delta C_P = 0.415 \pm 0.026$ J °C^{-1} g^{-1} in excellent agreement with the published 0.40 value [25].

Using the methodology described above for calculating the dynamic fragility based on Eqs. (1) and (2) (see Fig. 3 for lamotrigine), we obtained the values of

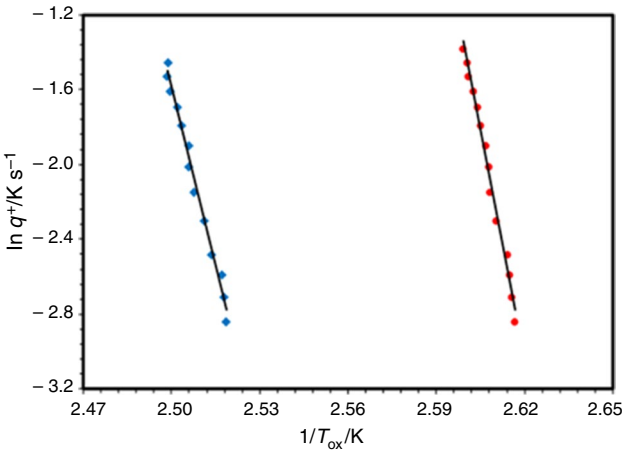

Fig. 3 Dynamic fragility of lamotrigine observed by DSC: "Arrhenius plots" of the logarithm of the heating rate, q^+, as a function of $1000/T_{ov}$ (diamonds, blue in the online edition) and of $1000/T_{on}$ (circles, red in the online edition), where T_{on} is the temperature of the extrapolated onset and T_{ov} is the temperature of the overshoot peak, of the glass transition signature on heating. The experiments were such that the ratio between the heating rate, q^+, and the previous cooling rate, q^-, was unity: $q^-/q^+ = 1$

Table 2 Properties of the glass transition and of the structural relaxation of bifonazole and lamotrigine

	Bifonazole		Lamotrigine	
	This work	Literature	This work	Literature
T_{gDSC}/°C	14[a]	14.6 [25]; 15.2 [47]; 16.1 [23]; 16.9 [26]	94[a]	–
T_{gTSDC}/°C	8	–	80	–
ΔC_P/J °C^{-1} g^{-1}	0.42 ± 0.03[b]	0.40 [25]	0.47 ± 0.01[c]	–
m_{DSC} (T_{ov})	61	–	72	–
m_{DSC} (T_{on})	73	76 [23]	89	–
m_{TSDC}	97	–	72	–

[a]Extrapolated onset temperature on heating at 10 °C min^{-1}

[b]Mean over 46 determinations

[c]Mean over 61 determinations

$E_a(T_{ov}) = 336$ kJ mol^{-1} and $E_a(T_{on}) = 402$ kJ mol^{-1} for the activation energy of the structural relaxation of bifonazole.

With these values in Eq. (2), we obtain $m_{DSC} = 61$ from T_{ov} and 73 from T_{on} (see Table 2). It should be noted that the determination of the onset of the stepwise signal of the glass transition at different heating rates was particularly difficult in the case of bifonazole, which resulted in a significant dispersion of the results and led to a greater number of experimental determinations.

Lamotrigine In the absence of published studies on the lamotrigine glass transition, the values of the dynamic properties presented below cannot be compared with others. The glass transition temperature measured by DSC was found at $T_{gDSC} = 94.3$ °C, and the heat capacity jump at the glass transition was $\Delta C_P = 0.468 \pm 0.014$ J °C^{-1} g^{-1}.

On the other hand, using the methodology described before, the activation energy of the structural relaxation of lamotrigine was found to be $E_a(T_{ov}) = 530$ kJ mol^{-1} and $E_a(T_{on}) = 655$ kJ mol^{-1} (see Fig. 3). With these values in Eq. (2), we obtained $m_{DSC} = 72$ from T_{ov} and 89 from T_{on} (see Table 2). Remember that the values of $E_a(T_g)$ and m_{DSC} obtained on the basis of the extrapolated onset temperature, T_{on}, are physically more credible because they are less distorted by aging.

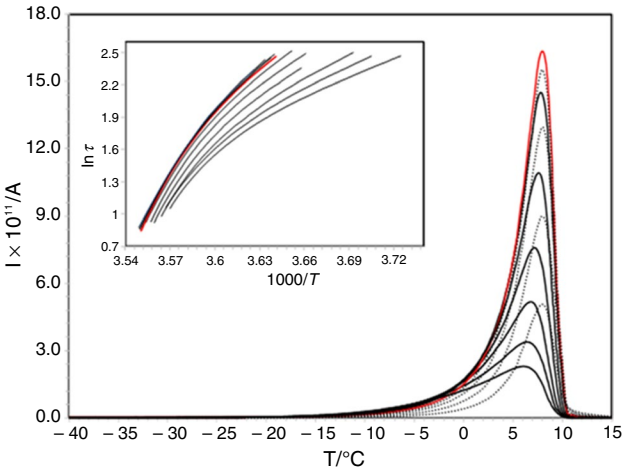

Fig. 4 Partial polarization peaks in the glass transformation region of bifonazole, obtained with polarization temperatures, T_P, from −7 to +9 °C. The PP peak with higher intensity (red in the online edition), obtained with $T_p = 5$ °C, is located at $T_M = (T_g)_{TSDC} = 8$ °C. The other experimental conditions were: strength of the polarizing electric field, $E = 350$ V mm^{-1}; polarization time, $t_P = 5$ min.; width of the polarization window, $\Delta T = 2$ °C; heating rate, $q = 6$ °C min^{-1}. The insert shows the $\tau(T)$ versus $1/T$ lines corresponding to the depolarization $I(T)$ peaks shown in the main figure; the thicker line, red in the online edition, is that which corresponds to the peak $I(T)$ of higher intensity, and it is from this line that the activation energy of structural relaxation, $E_a(T_M)$, and the dynamic fragility, m, are calculated

Thermally stimulated depolarization currents

The information presented above and collected by DSC on the dynamic fragility of our two glass-formers can be further elucidated by the TSDC technique. For this purpose, the temperature ranges of the amorphous solid state and of the glass transformation were scanned with partial polarization (or narrow polarization window) experiments.

The glass transformation region

Figure 4 shows some of the results obtained in the glass transition region of bifonazole; these are depolarization peaks, $I(T)$, obtained by partial polarization (or narrow polarization window) experiments, each corresponding to a narrowly distributed mobility. The general appearance of the figure is similar to that found in other glass-formers [48]: while the polarization window ΔT is within the temperature range of the amorphous solid, the partial polarization experiment is capable of retaining some polarization in the freezing step, which is depolarized on the next heating ramp giving rise to a depolarization current peak; in contrast, if the polarization window is in the liquid range, all the polarization created by the field in the polarization step will disappear when it is withdrawn, hence the relative configuration of the different depolarization peaks, with increasing area as the polarization window approaches T_g and with a sharply decreasing area when that temperature is reached and exceeded.

The peak with higher intensity in Fig. 4 (red in the online edition) has very special features; one is that the temperature of its maximum, T_M, corresponds to the glass transition temperature provided by TSDC, $T_M = T_{gTSDC}$ [48]; we thus have for bifonazole $T_{gTSDC} = 8$ °C, a value a little smaller than that obtained by DSC (see Table 2). Another feature of this peak, the most intense among the peaks of Fig. 4, is that it results from the depolarization of the motional modes of the structural relaxation with higher activation energy [48, 49]; for this reason, this depolarization peak is the one chosen for the calculation of the dynamic fragility in TSDC [14, 50].

The temperature-dependent relaxation time, $\tau(T)$, of each narrowly distributed mobility can be calculated from the raw experimental result, $I(T)$ (see supplementary data associated with Ref. [13] or appendix of Ref. [14]), and each $\tau(T)$ line contains the complete kinetic information about the respective motional mode. The $\tau(T)$ lines corresponding to the peaks of the main Fig. 4 are shown in the insert, and the thicker line (red in the online edition) corresponds to the highest intensity peak of the main figure. From the $\tau(T)$ line of the highest intensity peak, located at T_M in the glass transition region, we can easily calculate $E_a(T_M)$ and then the dynamic fragility, m_{TSDC}, from Eq. (2). The activation energy of the structural relaxation was found to

be $E_a(T_g) = 494$ kJ mol^{-1} for lamotrigine, and the fragility index, from Eq. (2), is $m_{TSDC} = 72$. Table 2 shows the values of the glass transition temperature, T_{gTSDC}, and of the dynamic fragility, m_{TSDC}, for the two systems studied.

All this kinetic information regarding the slow molecular motions in the amorphous solid state and in the glass transition can be condensed into a graph of $E_a(T_m)$ versus T_m, which is currently called "relaxation map," where each motional mode (corresponding to each depolarization peak $I(T)$) is characterized by its location on the temperature axis and by its activation energy. Figure 5 shows such a relaxation map for the two studied glass-forming liquids.

The results for the peaks $I(T)$ of Fig. 4, relative to the glass transition relaxation of bifonazole, correspond to some of the blue diamonds between 5 and 10 °C with activation energies in the range of 250 to 500 kJ mol^{-1}. In each group of points corresponding to a given glass-former in Fig. 5, the coordinates of the point with higher E_a can be used to estimate the dynamic fragility; we can qualitatively infer that the $E_a(T_M)$ value is close for bifonazole and lamotrigine, whereas the glass transition temperature is substantially higher in lamotrigine compared to bifonazole; it follows that given Fig. 5 and bearing in mind Eq. (2), the dynamic fragility of bifonazole is predictably higher than that of lamotrigine, which is confirmed by the values given in Table 2.

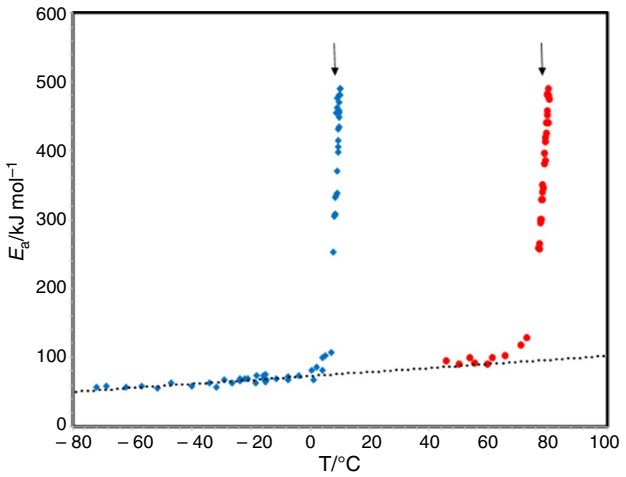

Fig. 5 TSDC relaxation map of the two studied glass-forming APIs: activation energy, $E_a(T_m)$, of the partial polarization components of the different relaxations as a function of the peak's location, T_m. The correspondence between the dots and the glass-formers is as follows: bifonazole (diamonds, blue in the online edition), and lamotrigine (circles, red in the online edition). The arrows indicate T_{gTSDC}, the glass transition temperature provided by TSDC. The dotted line describes the zero entropy behavior. The points in the proximity of the zero entropy line correspond to the local, secondary relaxations, while the points in the vicinity of T_{gTSDC}, displaying a strong and continuous deviation from that line, refer to the cooperative modes of the α-relaxation

The secondary relaxations

The partial polarization peaks obtained in the amorphous solid state showed very low dielectric strength in lamotrigine compared with bifonazole, which certainly arises from more active dipolar mobility in the amorphous solid state of this latter glass-former. Figure 6 shows some results of PP experiments carried out on the glassy bifonazole.

The points corresponding to the mobility modes of the secondary relaxations of our two glass-forming systems are shown in the relaxation map (Fig. 5) in the close vicinity of the dashed line, the so-called zero entropy line (ZEL) or Starkweather line [51–53]. The equation of this line can be written as:

$$\frac{1}{E_a} = \frac{rhN_A}{R^2T_m^3 e}\exp\left(\frac{E_a}{RT_m}\right) \quad (3)$$

with E_a in J mol^{-1} and T_m in K, and it defines an effective lower limit for the activation energy of the viscoelastic relaxations [53]; in Eq. (3) h, N_A and R are, respectively, the Planck, Avogadro and ideal gas constants, e is the Neper number, and r is the heating rate of the depolarization ramp of the TSDC experiment. The zero entropy line is obtained by equating the Arrhenius and Eyring equations and considering the Eyring's activation entropy equal to zero: $\Delta S^{\neq} = 0$ (see Supplementary Materials for an explanation of the rationale for Eq. (3)); this imposition of a zero activation entropy corresponds to setting the lower limit of the activation energy of the viscoelastic relaxations.

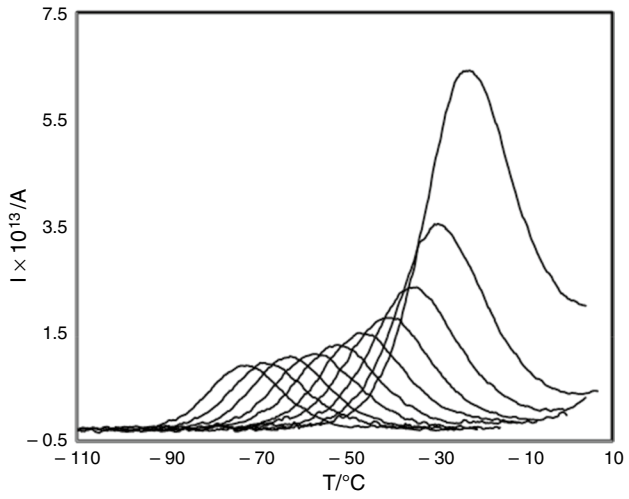

Fig. 6 Partial polarization peaks of the secondary mobility of bifonazole. The experimental conditions were: heating rate, $q = 4$ °C min^{-1}, strength of the polarizing electric field, $E = 350$ V mm^{-1}; polarization time, $t_P = 5$ min.; width of the polarization window, $\Delta T = 2$ °C; the polarization temperatures of the different experiments varied from −75 to −30 °C every five degrees

The dependence $E_a(T_m)$ described in Eq. (3) is almost linear over a relatively wide temperature range (see Supplementary Materials) which allows us to use as a reasonable approximation of the zero entropy line the equation:

$$E_{ZEL} = 37RT_m \quad (4)$$

for a heating rate of 4 °C min^{-1} and in the temperature range between 65 and 425 K. Looking at the relaxation map of Fig. 5, we find that the motional modes of the bifonazole secondary relaxation (Fig. 6) have activation energies between ~ 55 and ~ 75 kJ mol^{-1} and are detected in the wide temperature range from − 75 to + 5 °C; lamotrigine's secondary motional modes, on the other hand, are only detected in the very close proximity of the glassy transformation, in the narrow range between 50 and 75 °C, and show activation energies between ~ 87 and ~ 97 kJ mol^{-1}. In fact, lamotrigine has a rigid molecular structure that does not allow changes in the orientation of dipolar parts of the molecule in relation to each other. In bifonazole, the stiffness is not as strong, as the benzyl-imidazole moiety can rotate around the carbon–carbon bond that connects it to the biphenyl fraction. In addition, there are intermolecular hydrogen bonds in lamotrigine, which is not the case with bifonazole. These differences in the occurrence of secondary relaxations result, at least in part, from the differences between the two glass-forming substances in terms of molecular rigidity and intensity of intermolecular interactions. It is important to note that all the relaxations detected by TSDC below the glass transition region are found to obey the zero entropy line, i.e., have activation energies given by Eq. (4) and zero activation entropy (Arrhenius pre-factor $\tau_0 = 10^{-13}$–10^{-14} s or, in terms of frequency, $f_0 = 10^{12}$–10^{13} Hz). This is so for very different glass-formers, both polymeric [54, 55] and low molecular mass [56–59], and also for positionally or orientationally disordered glasses [46, 60] and for ionic liquids [61, 62]. However, studies of the secondary molecular mobility in the amorphous solid state, in particular those of dielectric relaxation spectroscopy (DRS), show the existence of various types of motion [63] with distinct signatures, namely with kinetics where the pre-exponential Arrhenius factor differs significantly from $\tau_0 = 10^{-13}$ s. So far, there is no attempt in the literature to reconcile the two dielectric techniques, i.e., to explain the apparent divergence of their results with regard to secondary relaxations; we believe we can look into this matter in the near future. Note finally that introducing Eq. (4) into the definition of the dynamic fragility (Eq. (2)) leads to $m = 16$ which is the limiting value of dynamic fragility for very strong glasses (see Section "The glass transition and the dynamic fragility"); the dynamic fragility of a glass-forming system thus appears in TSDC as proportional to the departure (at T_g) of the points of α-relaxation from the zero entropy line.

Conclusions

The thermal behavior and polymorphism of bifonazole and lamotrigine were investigated by DSC. Both are easily amorphizable by cooling from the liquid and both undergo cold crystallization. A polymorph of bifonazole not yet reported in the literature was obtained by cold crystallization; in contrast, no clear evidence of lamotrigine polymorphism was found: In this case, we only reported observations that cast suspicion on the possible existence of polymorphism. DSC was also used to study the glass transition by determining its temperature, T_g, activation energy $E_a(T_g)$ (and dynamic fragility, m_{DSC}) as well as the associated heat capacity jump, $\Delta C_p(T_g)$.

The TSDC study provided experimental values of the glass transition temperature, T_{gTDSC}, and of the dynamic fragility, m_{TSDC}, in reasonable agreement with those obtained by DSC. A secondary relaxation was also characterized by TSDC. The absence of other dynamic studies on these glass-formers does not allow the comparison of our results with those of other techniques, namely with dielectric spectroscopy. On the other hand, attention was drawn to the general need to understand in their mutual relationship the TSDC and DRS results on the secondary relaxations.

Acknowledgements This work was partially supported by Fundação para a Ciência e a Tecnologia (FCT), Portugal, Project UIOB/00100/2020.

Compliance with ethical standards

Conflict of interest The authors declare no conflict of interest.

References

1. Lackner TE, Clissold SP. Bifonazole. Drugs. 1989;38:204–25.
2. Fitton A, Goa KL. Lamotrigine. Drugs. 1995;50:691–713.
3. Taylor LS, Shamblin SL. Amorphous solids. In: Brittain HG, editor. Polymorphism and pharmaceutical solids. Drugs and the pharmaceutical sciences, vol. 192. New York: Informa Healthcare; 2009. p. 587–629.
4. Murdande SB, Pikal MJ, Shanker RM, Bogner RH. Solubility advantage of amorphous pharmaceuticals: II. Application of quantitative thermodynamic relationships for prediction of solubility enhancement in structurally diverse insoluble pharmaceuticals. Pharm Res. 2010;27:2704–14.
5. Murdande SB, Pikal MJ, Shanker RM, Bogner RH. Solubility advantage of amorphous pharmaceuticals: I. A thermodynamic analysis. J Pharm Sci. 2010;99:1254–64.
6. Johari GP, Shanker RM. On the solubility advantage of a pharmaceutical's glassy state over the crystal state, and of its crystal polymorphs. Thermochim Acta. 2014;598:16–27.
7. Shamblin SL, Tang X, Chang L, Hancock BC, Pikal MJ. Characterization of the time scales of molecular motion in pharmaceutical important glasses. J Phys Chem B. 1999;103:4113–21.

8. Kothari K, Ragoonanan V, Suryanarayanan R. Influence of molecular mobility on the physical stability of amorphous pharmaceuticals in the supercooled and glassy states. Mol Pharm. 2014;11:3048–55.
9. Bhattacharya S, Suryanarayanan R. Local mobility in amorphous pharmaceuticals-characterization and implications on stability. J Pharm Sci. 2009;98:2935–53.
10. Xu Y, Carpenter JF, Cicerone MT, Randolph TW. Contributions of local mobility and degree of retention of native secondary structure to the stability of recombinant human growth hormone (rhGH) in glassy lyophilized formulations. Soft Matter. 2013;9:7855–65.
11. Lu J, Rohani S. Polymorphism and crystallization of active pharmaceutical ingredients (APIs). Current Med Chem. 2009;16:884–905.
12. Moura Ramos JJ, Taveira-Marques R, Diogo HP. Estimation of the fragility index of indomethacin by DSC using the heating and cooling rate dependency of the glass transition. J Pharm Sci. 2004;93:1503–7.
13. Diogo HP, Viciosa MT, Moura Ramos JJ. Differential scanning calorimetry and thermally stimulated depolarization currents study on the molecular dynamics in amorphous fenofibrate. Thermochim Acta. 2016;623:29–35.
14. Moura Ramos JJ, Viciosa MT, Diogo HP. Thermal behaviour of two anti-inflammatory drugs (celecoxib and rofecoxib) and slow relaxation dynamics in their amorphous solid state. Comparison between the dynamic fragility obtained by dielectric spectroscopy and by thermostimulated currents. Mol Phys. 2018;117:644–60.
15. van Turnhout J. Thermally stimulated discharge of polymer electrets. Amsterdam: Elsevier; 1975.
16. Chen R, Kirsh Y. Analysis of thermally stimulated processes. Oxford: Pergamon Press; 1981.
17. van Turnhout J. Thermally stimulated discharge of electrets. In: Sessler GM, editor. Electrets. Topics in applied physics, vol. 33. Berlin: Springer; 1987. p. 81–215.
18. Gun'ko VM, Zarko VI, Goncharuk EV, Andriyko LS, Turov VV, Nychiporuk YM, Leboda R, Skubiszewska-Zieba J, Gabchak AL, Osovskii VD, Ptushinskii YG, Yurchenko GR, Mishchuk OA, Gorbik PP, Pissis P, Blitz JP. TSDC spectroscopy of relaxational and interfacial phenomena. Adv Colloid Interface Sci. 2007;131:1–89.
19. Sauer BB. Thermally stimulated currents: recent developments in characterisation and analysis of polymers. In: Cheng SZD, editor. Applications to polymers and plastics. Handbook of thermal analysis and calorimetry, vol. 3. Amsterdam: Elsevier; 2002. p. 653–711.
20. Vassilikou-Dova A, Kalogeras IM. Dielectric analysis (DEA). In: Menczel JD, Prime RB, editors. Thermal analysis of polymers: fundamentals and applications. Hoboken: Wiley; 2009. p. 497–613.
21. Boutonnet-Fagegaltier N, Lamure A, Menegotto J, Lacabanne C, Caron A, Duplaa H, Bauer M. The use of thermally stimulated current spectroscopy in the pharmaceutical sciences. In: Craig DQM, Reading M, editors. Thermal analysis of pharmaceuticals. Boca Raton: CRC Press; 2007. p. 359–82.
22. Barker S, Antonijevic MD. Thermal analysis—dielectric techniques. In: Storey RA, Ymén I, editors. Solid state characterization of pharmaceuticals. Chichester: Blackwell Publishing; 2011. p. 187–206.
23. Kawakami K, Harada T, Yoshihashi Y, Yonemochi E, Terada K, Moriyama H. Correlation between glass-forming ability and fragility of pharmaceutical compounds. J Phys Chem B. 2015;119:4873–80.
24. Morin N, Chilouet A, Millet J, Rouland JC. Bifonazole-β-cyclodextrin inclusion complexes thermal analysis and X-ray powder diffraction study. J Therm Anal Calorim. 2000;62:187–201.
25. Domanska U, Pobudkowska A, Pelczarska A, Winiarska-Tusznio M, Gierycz P. Solubility and pKa of select pharmaceuticals in water, ethanol, and 1-octanol. J Chem Thermodyn. 2010;42:1465–72.
26. Trasi NS, Baird JA, Kestur US, Taylor LS. Factors influencing crystal growth rates from undercooled liquids of pharmaceutical compounds. J Phys Chem B. 2014;118:9974–82.
27. Morin N, Crini G, Cosentino C, Millet J, Vebrel J, Rouland JC. Formation of two particular structures between β-cyclodextrin and bifonazole: β-cyclodextrin-bifonazole and (β-cyclodextrin)-bifonazole (where $2 < i < 3$). J Chem Soc Perkin Trans. 1999;2:2647–51.
28. Kelemen H, Csillag A, Hancu G, Székely-Szentmiklósi B, Fulöp I, Varga E, Grama L, Orgován G. Characterization of inclusion complexes between bifonazole and different cyclodextrins in solid and solution state. Macedon J Chem Chem Eng. 2017;36:81–91.
29. Trandafirescu C, Gyéresi Á, Szabadai Z, Kata M, Aigner Z. Solid-state characterization of bifonazole-β-cyclodextrin binary systems. Note I. Farmacia. 2014;62:521–31.
30. Évora AOL, Castro RAE, Maria TMR, Ramos Silva M, Canotilho J, Eusébio ME. Lamotrigine: design and synthesis of new multicomponent solid forms. Eur J Pharm Sci. 2019;129:148–62.
31. Thipparaboina R, Kumar D, Mittapalli S, Balasubramanian S, Nangia A, Shastri NR. Ionic, neutral, and hybrid acid-base crystalline adducts of lamotrigine with improved pharmaceutical performance. Cryst Growth Des. 2015;15:5816–26.
32. Rahman Z, Zidan AS, Samy R, Sayeed VA, Khan MA. Improvement of physicochemical properties of an antiepileptic drug by salt engineering. AAPS PharmSciTech. 2012;13:793–801.
33. Leksic E, Pavlovic G, Mestrovic E. Cocrystals of lamotrigine based on coformers involving carbonyl group discovered by hot-stage microscopy and DSC screening. Cryst Growth Des. 2012;12:1847–58.
34. Chadha R, Saini A, Arora P, Jain DS, Dasgupta A, Guru Row TN. Multicomponent solids of lamotrigine with some selected coformers and their characterization by thermoanalytical, spectroscopic and X-ray diffraction methods. CrystEngComm. 2011;13:6271–84.
35. Chadha R, Saini A, Khullar S, Jain DS, Mandal SK, Guru Row TN. Crystal structures and physicochemical properties of four new lamotrigine multicomponent forms. Cryst Growth Des. 2013;13:858–70.
36. Beattie K, Phadke G, Novakovic J. Lamotrigine. In: Brittain HG, editor. Profiles of drug substances, excipients and related methodology, vol. 37. Waltham: Academic Press; 2012. p. 245–85.
37. Parmar KR, Patel KA, Shah SR, Sheth NR. Inclusion complexes of lamotrigine and hydroxy propyl β-cyclodextrin: solid state characterization and dissolution studies. J Incl Phenom Macro Chem. 2009;65:263–8.
38. Patel MB, Valand NN, Modi NR, Joshi KV, Harikrishnan U, Kumar SP, Jasrai YT, Menon SK. Effect of p-sulfonatocalix[4] resorcinarene (PSC[4]R) on the solubility and bioavailability of a poorly water soluble drug lamotrigine (LMN) and computational investigation. RSC Adv. 2013;3:15971–81.
39. Shinde VR, Shelake MR, Shetty SS, Chavan-Patil AB, Pore YV, Late SG. Enhanced solubility and dissolution rate of lamotrigine by inclusion complexation and solid dispersion technique. J Pharm Pharmacol. 2008;60:1121–9.
40. Moynihan CT, Easteal AJ, Wilder J, Tucker J. Dependence of the glass transition temperature on heating and cooling rate. J Phys Chem. 1974;78:2673–7.
41. Moynihan CT, Lee S-K, Tatsumisago M, Minami T. Estimation of activation energies for structural relaxation and viscous flow from DTA and DSC experiments. Thermochim Acta. 1996;280–281:153–62.

42. Crowley KJ, Zografi G. The use of thermal methods for predicting glass-former fragility. Thermochim Acta. 2001;380:79–93.
43. Svoboda R. How to determine activation energy of glass transition. J Therm Anal Calorim. 2014;118:1721–32.
44. Svoboda R, Málek J. Description of enthalpy relaxation dynamics in terms of TNM model. J Non-Cryst Solids. 2013;378:186–95.
45. Moura Ramos JJ, Diogo HP. Orientational glass, orientationally disordered crystal and crystalline polymorphism: a further study on the thermal behavior and molecular mobility in levoglucosan. J Mol Liq. 2019;286:110914.
46. Böhmer R, Ngai KL, Angell CA, Plazek DJ. Nonexponential relaxations in strong and fragile glass formers. J Chem Phys. 1993;99:4201–9.
47. Kestur US, Van Eerdenbrugh B, Taylor LS. Influence of polymer chemistry on crystal growth inhibition of two chemically diverse organic molecules. CrystEngComm. 2011;13:6712–8.
48. Moura Ramos JJ, Diogo HP. The determination of the glass transition temperature by thermally stimulated depolarization currents. Comparison with the performance of other techniques. Phase Transit. 2017;90:1061–78.
49. Moura Ramos JJ, Correia NT. The Deborah number, relaxation phenomena and thermally stimulated currents. Phys Chem Chem Phys. 2001;3:5575–8.
50. Diogo HP, Viciosa MT, Moura Ramos JJ. Thermally Stimulated Currents: principles, methods for data processing and significance of the information provided. Suppl Data Thermochim Acta. 2016;623:29–35. https://doi.org/10.1016/j.tca.2015.11.012.
51. Starkweather HW. Simple and complex relaxations. Macromolecules. 1981;14:1277–81.
52. Starkweather HW. Noncooperative relaxations. Macromolecules. 1988;21:1798–802.
53. Starkweather HW. Aspects of simple, non-cooperative relaxations. Polymer. 1991;32:2443–8.
54. Moura Ramos JJ, Mano JF, Sauer BB. Some comments on the significance of the compensation effect observed in thermally stimulated current experiments. Polymer. 1997;38:1081–9.
55. Pinto SS, Moura Ramos JJ, Diogo HP. The slow molecular mobility in poly(vinyl acetate) revisited: new contributions from thermally stimulated currents. Eur Polym J. 2009;45:2644–52.
56. Correia NT, Moura Ramos JJ, Descamps M, Collins G. Molecular mobility and fragility in indomethacin: a thermally stimulated depolarisation currents study. Pharm Res. 2001;18:1767–74.
57. Moura Ramos JJ, Correia NT, Diogo HP. Vitrification, nucleation and crystallization in phenyl-2-hydroxybenzoate (salol) studied by differential scanning calorimetry (DSC) and thermally stimulated depolarisation currents (TSDC). Phys Chem Chem Phys. 2004;6:793–8.
58. Moura Ramos JJ, Diogo HP. The slow relaxation dynamics in active pharmaceutical ingredients studied by DSC and TSDC: voriconazole, miconazole and itraconazole. Int J Pharm. 2016;501:39–48.
59. Moura Ramos JJ, Piedade MF, Diogo HP, Viciosa MT. Thermal behavior and slow relaxation dynamics in amorphous efavirenz: a study by DSC, XRPD, TSDC, and DRS. J Pharm Sci. 2019;108:1254–63.
60. Moura Ramos JJ, Diogo HP. Phase behavior and slow molecular dynamics in the glassy state and in the glass transformation of a nematic liquid crystal: 4CFPB. Liq Cryst. 2020;47:604–17.
61. Diogo HP, Pinto SS, Moura Ramos JJ. Slow molecular mobility in the amorphous solid and the metastable liquid states of three 1-alkyl-3-methylimidazolium chlorides. J Mol Liq. 2013;178:142–8.
62. Viciosa MT, Diogo HP, Moura Ramos JJ. The ionic liquid BmimBr: a dielectric and thermal characterization. RSC Adv. 2013;3:5663–72.
63. Ngai KL, Paluch M. Classification of secondary relaxation in glass-formers based on dynamic properties. J Chem Phys. 2004;120:857–73.